Optimization of Charging Strategies for Battery Electric Vehicles under Uncertainty

Huber, Gerhard; Bogenberger, Klaus; Van Lint, Hans

DOI
10.1109/TITS.2020.3027625

Publication date
2022

Document Version
Final published version

Published in
IEEE Transactions on Intelligent Transportation Systems

Optimization of Charging Strategies for Battery Electric Vehicles Under Uncertainty

Gerhard Huber, Klaus Bogenberger, and Hans van Lint

***Abstract*—The comparably low driving ranges of battery electric vehicles (BEV) cause time-consuming recharging stops if long distances have to be covered. Thus, navigation systems not only have to compute routes leading from the BEV's current position to the destination, but also to plan recharging stops. This type of routing problem is often modeled as a constrained shortest path problem. The constraint ensures that the BEV does not run out of energy. In this paper, a de facto deterministic reformulation of this problem type is suggested, which allows handling uncertainty–particularly the risks resulting from imperfect energy consumption predictions. For this purpose, a certain part of the battery capacity is used as an energy buffer. Different approaches to dynamically optimize the size of this energy buffer in dependency of the expected level of uncertainty are proposed and a corresponding modification of a typical routing algorithm is described. Furthermore, a simulation study is conducted showing that the described framework allows keeping the probability to run out of energy close to zero (for the test settings: < 0.5%) as long as a suitable approach for defining the size of the energy buffer is applied.**

***Index Terms*—Battery electric vehicle, shortest path problem, uncertainty, routing.**

I. Introduction

THE World Health Organization estimated that air pollution was responsible for seven million premature deaths in 2012 [1]. To improve the situation especially in urban areas, alternatives to internal combustion engine vehicles (ICEV) have gained relevance. Besides fuel cell vehicles, particularly battery electric vehicles (BEV) are named as one of the most promising technologies. However, BEV selling numbers remain low in many countries. The so-called **range-anxiety**–the deeply rooted fear of potential customers to run out of energy while driving a BEV–is seen as one of the main reasons for the limited demand for BEVs (see p. 10 in [2]). Range-anxiety primarily results from the typically sparse charging infrastructure in combination with the, compared to ICEVs, low driving range of BEVs [3]. Building up additional charging infrastructure is an expensive and time-consuming process. The driving ranges of BEVs have been increased during the last years, but there is still a significant gap to the driving ranges achieved by ICEVs. In this paper, a third approach to tackle range-anxiety is pursued.

According to [3], a well-informed driver of a BEV, i.e., someone who receives recent and reliable information about the remaining driving range and nearby charging possibilities, is less vulnerable to range-anxiety. There exists a variety of approaches to ensure that drivers feel well-informed. In this work, the focus will be set on computing **charging strategies** for BEVs. Given a road network and some charging infrastructure placed along the network, the BEV's current position, its current state of charge and a destination, a charging strategy is in the following defined as a sequence of instructions which describes

- a route from the current location to the destination
- at which charging stations along this route the BEV has to be recharged
- up to which state of charge the battery of the BEV has to be recharged at the respective charging station.

Charging strategies have to be reliable, i.e., the risk that a BEV which follows a charging strategy runs out of energy before the destination is reached has to be kept as low as possible. Reliability is essential to reduce or, in the best case, eliminate range-anxiety. Second, a charging strategy has to be efficient, i.e., unnecessary and unnecessarily long charging stops have to be avoided. If charging strategy recommendations are too conservative, then the travel times resulting when following these strategies will in general be very high. It is likely that drivers of BEVs will stop relying on such recommendations, since they soon will be able to do better on their own.

Clearly, reliability and efficiency, the way they are described here, are opposing obstacles. The central motivation of this paper, which is based on a PhD thesis [4], is to show how dynamic optimization algorithms can be adjusted in order to achieve a reasonable compromise between reliability and efficiency. For this purpose, we start in section II with a literature review and describe an already existing formulation of the problem of finding optimal charging strategies as a shortest path problem (SPP). In section III, a novel generic approached is proposed which modifies this formulation in order to address the existence of uncertainty. Several ideas to concretize this

Manuscript received January 10, 2020; revised July 11, 2020; accepted September 8, 2020. Date of publication October 15, 2020; date of current version February 2, 2022. This work was supported in part by the Federal Ministry for the Environment, Nature Conservation, Building, and Nuclear Safety (Research Project PREMIUM), German and in part by the Federal Ministry of Transport and Digital Infrastructure (Research Project DC-Ladestation am Olympiapark), German. The Associate Editor for this article was S. A. Birrell. *(Corresponding author: Gerhard Huber.)*

Gerhard Huber is with the Department of Civil Engineering, Fakultät für Bauingenieurwesen und Umweltwissenschaften, Universität der Bundeswehr München, 85577 Neubiberg, Germany (e-mail: huber.gerhard4@googlemail.com).

Klaus Bogenberger is with the Department of Traffic Engineering and Control, Technical University of Munich, 80333 Munich, Germany (e-mail: klaus.bogenberger@unibw.de).

Hans van Lint is with the Transport and Planning Department, Faculty of Civil Engineering, Delft University of Technology, 2600 GA Delft, The Netherlands (e-mail: j.w.c.vanlint@tudelft.nl).

Digital Object Identifier 10.1109/TITS.2020.3027625

generic approach are sketched. A corresponding optimization algorithm is described in section IV. It can be understood as an example of how dynamic optimization algorithms can be adjusted to handle uncertainties. In section V, two of the suggested approaches are tested within a simulation study. In this study, a BEV follows frequently updated charging strategies, which are based on imperfect information about the future traffic situation. The difference between the predicted and the real traffic situation causes uncertainty within the simulation. It is analysed in detail, under which conditions which of the proposed algorithms performs best. The paper ends in section VI with a short summary of the contributions of the paper.

II. State of the Art

When it comes to routing problems for BEVs, there exists a vast literature about deriving adequate energy consumption models for BEVs. Physical consumption models are typically applied in this context [5] [6]. Such models take a variety of vehicle parameters (frontal area, vehicle mass, etc.) into account to determine driving resistance (which consists of rolling resistance, aerodynamic resistance, climbing resistance and inertial resistance) in dependency of driving speed, acceleration and road steepness. Based on the driving resistance, the mass of the BEV and the energy conversion efficiency of the electric motor, the energy which is necessary to move and accelerate the BEV is estimated. The focus is usually set on the influence of weather conditions [7] and road steepness [8] [9]. The latter is particularly interesting, because of the BEVs ability to regain energy via recuperation, i.e., BEVs can recharge their battery by making use of the negative climbing resistance when driving downhill. Routing problems are often modeled as SPPs and the possibility to recharge the battery leads to negative edges costs within these models. Many algorithms which are widely used to solve SPPs, such as Dijkstra's algorithm [10], are not able to ensure the computation of optimal solutions if edge costs are partly negative. To overcome this issue, so-called label correction algorithms, like the algorithm of Floyd and Warshall [11], can be applied. Alternatively, Johnson [12] suggested a method that makes it possible to modify the edge costs of a graph in such a way that no longer negative edge costs occur. At the same time, this method ensures that the set of shortest paths leading from any starting to any destination node is the same as it was before the modification. Former works on energy-efficient routing [8] [9] [13], i.e., routes have to be computed which minimize total energy consumption, are often based on the method of Johnson.

According to the introduction, charging strategies consist not only of route recommendations, but also of charging recommendations. The former is important for both BEVs and ICEVs. The latter is more critical for BEVs. Nevertheless, before the problem of finding optimal charging strategies arose, some papers already treated the so-called vehicle refueling problem [14]–[16]. The situation is basically the same as for the problem of finding optimal charging strategies, except that typically fuel costs have to be minimized and that the costs for fuel differ among the available gas stations.

Transferring the vehicle refueling problem from ICEVs to BEVs leads to what is from here on denoted as the problem of finding optimal charging strategies. One of the first paper published in this context is [17]. The problem of finding optimal charging strategies is modeled as an SPP. A charging station is represented by a single node on a graph. Paths on this graph are interpreted as charging strategies. If a path leads from a node A to a node B, while covering some of the nodes which represent charging stations, then the corresponding charging strategy suggests to follow the route described by the path and to fully recharge the battery of the BEV whenever one of the charging nodes is reached. The energy for passing edges of the graph is assumed to depend linearly on the length of the road segments which are represented by these edges. The travelled distance or total travel times, i.e., the time for driving plus the time for recharging, are used as the optimization criterion. The optimization itself is basically done in two steps : In a pre-processing step, an auxiliary graph is constructed. This graph consists only of nodes representing the given charging stations and artificially constructed edges connecting these stations. The actual shortest path search can be interpreted as a hierarchical modification of Dijkstra's algorithm. It starts on the original graph and is lifted, as soon as possible, to the auxiliary graph. When the search gets close to the destination, then the algorithm returns to the original graph. This procedure improves computation times significantly. In [18], an approach comparable to one from Kobayashi is pursued. The problem of finding optimal charging strategies is again modeled as an SPP and it is only possible to fully recharge a battery when reaching a charging station. Furthermore, also a pre-processing step is conducted to improve computation times. However, the amount of energy that is necessary to get from one node to another is calculated and stored for all pairs of nodes for which at least one of both nodes represents a charging station. Another difference to Kobayashi is that instead of travel times or travelled distance, solely energy consumption costs are considered and minimized. In [19], the framework described in [18] is further extended. The optimization of the charging strategies is now intended to find a compromise between consumed energy, travel time and travelled distance.

In [20], the weighted constrained shortest path problem with replenishment arcs is introduced. The focus is set on computational experiments on large networks. Reasonable computational speed is achieved on these large instances, similarly to [17] or [18], by making use of a preprocessing method. In [21] the minimum cost path problem with relays is decribed. A path on a graph is a solution to this type of SPP if the sum of the costs along a path does not exceed a given upper bound. In this context, some of the nodes of the considered graph are assumed to be relays. Whenever a path reaches such a node, the sum of edge costs is set back to zero. Thus, relays can be understood as recharging possibilities. In [22], the problem of finding optimal charging strategies is modeled as a dynamic program and solved via a backward recursion. In contrast to the previously mentioned works, not only a full recharging can be recommended, but recharging up to any state of charge between 0% and 100% is possible. The additional flexibility increases the optimization potential.

However, two unrealistic assumptions are made to achieve this: First, it is assumed that the BEV can be recharged at each node of a given graph. Second, the possible existence of negative edge costs due to recuperation is ignored. In [23] and [24], the problem of finding optimal charging strategies is described as a mixed integer nonlinear program. It is explained how this original problem formulation can be separated into two linear programs, which can be solved sequentially and very efficiently. Analogously to [22], solutions of the described optimization problem are able to recommend arbitrary recharging amounts.

Also the authors of this paper have contributed to the topic of computing optimal charging strategies [25], [26]. The problem itself is again modeled as an SPP. The most significant difference to the already mentioned approaches is that edge costs are not modeled as static quantities. Instead, edge costs describing the time and the energy that is necessary to pass road segments are assumed to be time-dependent. This allows taking the effect of dynamic factors, such as changing weather and traffic conditions, on energy consumption and travel times into account. In the following, the model described in [25] and [26] will be used as a basis for all further developments. A detailed description of this model can be found in section II-A. Please note that Wang suggested a very similar approach for modeling the problem of finding optimal charging strategies [27]. In this work, two algorithms which are both based on the A^*-algorithm are tested and compared.

Significantly different to the aforementioned contributions is the work of [28]. There, the stochastic optimal path problem with relays is proposed. Driving speeds and energy consumption are interpreted as random variables. The huge advantage of this approach is that the problem formulation allows taking only those charging strategies into account, which ensure a pre-defined minimal arrival probability. Two different label-correcting algorithms in combination with a preprocessing method are suggested to solve the problem. Though some simplifications are presumed–such as allowing only a full recharging, presuming that no correlations exist between random variables belonging to different edges, and ignoring that driving speeds and energy consumption may depend on time–the suggested algorithms are tested only on a small network. Due to the extremely high computational effort, this is typically done when solving stochastic routing problems. In the context of energy-efficient routing, some further works (besides [28]) exist that treat the topic of uncertainty [29] [30], but these contributions do not consider the possibility to recharge.

For completeness, it shall also be mentioned at this point that, besides providing charging strategies to a single BEV, situations in which a whole fleet of BEVs needs to be managed are also covered in research [31]–[33]. The main challenge for this type of problem usually is to ensure that each BEV reaches its destination as quickly as possible while only a limited number of charging stations is available. Clearly, it is more complicated to optimize charging strategies for a whole fleet of vehicles than for a single BEV. This fact has influence on the structure and complexity of the corresponding optimization problems and, along with this, also on the solution approaches which can be applied. If fleets of BEVs have to be coordinated, then quickly rising computation times often make it impossible to use optimization algorithms for big problem instances or necessitate keeping problem formulations quite simple.

A. Charging Strategy Optimization as a Shortest Path Problem

In the following, the problem of finding optimal charging strategies is modeled as an SPP. The construction of this optimization problem is separated into three parts: First, a graph that allows representing not only a road network, but also charging possibilities and charging strategies is introduced. Second, edge cost functions which decribe energy consumption and travel times for a BEV moving through a road network are derived. Third, a corresponding SPP is defined. Optimal solutions of this SPP can be interpreted as charging strategies, but the existence of uncertainty is still not addressed.

1) Graph Representation of Road Networks and Charging Processes: The fundament of an SPP is a mathematical graph. This graph has to represent the considered road network, where road segments are typically embodied by edges and junctions by nodes. For the problem of finding optimal charging strategies, the charging infrastructure and the available charging options have to be represented, too. The term "charging options" is intended to describe the set of all possible recommendations that can be made to a driver of a BEV when reaching a charging station. This can either be to charge up to a certain state of charge (we will from here on refer to a recommended state of charge as the "target state of charge") or to continue the trip without recharging. In this work, we follow the approach suggested in [26] to represent charging stations and charging options within a mathematical graph. For this purpose, let $K \in \mathbb{N}$ denote the number of charging stations located along the considered road network. For each of these charging stations, two additional nodes v_k^a and v_k^b are introduced, where $k \in \{1, 2, \ldots, K\}$ is used to indicate that these nodes belong to the k-th charging station. Node v_k^a marks the location of the junction at which the original road network can be left in order to get to the k-th charging station, v_k^b analogously embodies the location of the junction at which one can return to the original road network. To model the k-th charging station itself, a node v_k^i ("i" for "in") and a node v_k^o ("o" for "out") are added. Edge (v_k^a, v_k^i) is used to embody the way from the original road network to the charging station and edge (v_k^o, v_k^b) for the way back. A parameter $\Delta \in [0, 1]$ is introduced to model all possible charging options. This parameter defines the set of target states of charge. For example, if Δ is set equal to $0.05 = 5\%$, then it is later on possible to recommend charging up to any state of charge that is a multiple of 5%. Finally, a node $v_k^{l \cdot \Delta}$ and two edges $(v_k^i, v_k^{l \cdot \Delta})$ and $(v_k^{l \cdot \Delta}, v_k^o)$ are added for each $l \in \mathbb{N}$ which fulfills the following condition:

$$0\% \leq l \cdot \Delta \leq 100\% \tag{1}$$

The resulting graph is from here on denoted as $\vec{G}^{\Delta} = (V^{\Delta}, \vec{E}^{\Delta})$, where V^{Δ} represents the set of nodes and $\vec{E}^{\Delta}$ the set of edges. An example for such a graph is shown in Figure 1.

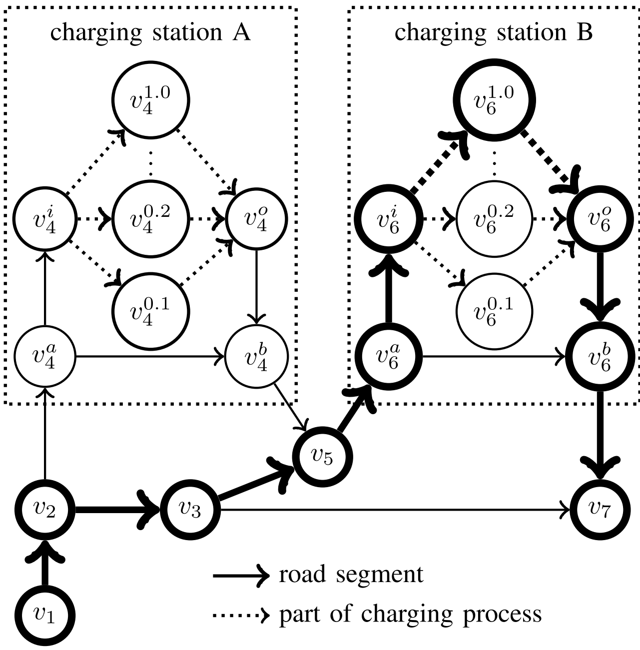

Fig. 1. Graph-based model of charging possibilities.

Dotted edges are used to represent parts of potential charging processes, whereas all other edges represent road segments. The path $[v_1, v_2, v_3, v_5, v_6^a, v_6^i, v_6^{1.0}, v_6^o, v_6^b, v_7]$, which consists of the bold edges and nodes in Figure 1, is intended to illustrate how paths on a graph $\vec{G}^\Delta$ can be interpreted as charging strategies: A path basically represents, as it is usually the case for SPPs, a route recommendation leading from its starting node to its last node. Moreover, whenever a path covers a node $v_k^{l\cdot\Delta}$, then the charging strategy which is encoded by this path suggests to recharge the battery at the k-th charging station up to a target state of charge of $l \cdot \Delta$. This means that the bold path in Figure 1 can be associated with a charging strategy suggesting to drive from the starting location v_1 directly to junction v_3 and then turn left to junction v_5. There, the driver of the BEV has to turn right and recharge up to a state of charge of $1.0 = 100\%$ at charging station B before continuing the trip until destination node v_7 is reached.

2) Modeling Travel Time and Energy Consumption: Here, the optimization of charging strategies is done with respect to total travel time, i.e., the time needed for driving and recharging when following a recommended charging strategy has to be minimized. This ensures that the number of charging stops is kept low, but it also makes it inevitable to introduce an edge cost functions c_T, which assigns time costs to edges. To simplify the following definitions, let $\vec{E}_{cs}^\Delta \subset \vec{E}^\Delta$ define the set of all edges representing parts of charging processes. The time costs for passing road segments are assumed to be time-dependent. For a given arrival time t_{arl} and for an edge $e \in \vec{E}^\Delta \setminus \vec{E}_{cs}^\Delta$, this means:

$$c_T(e, t_{arl}) = \text{time for passing segment } e \text{ at time } t_{arl} \quad (2)$$

For edges representing parts of a charging process, the corresponding time costs depend on the state of charge $SOC \in [0, 1]$ when arriving at the charging station and on the target state of charge $l \cdot \Delta \in [0, 1]$:

$$\begin{aligned} c_T\left((v_k^{l\cdot\Delta}, v_k^o), SOC\right) &= \text{time to recharge} \\ &\quad\ \text{from } SOC \text{ to } l \cdot \Delta \\ c_T\left((v_k^i, v_k^{l\cdot\Delta}), SOC\right) &= 0 \end{aligned}$$

Besides minimizing total travel times, it also has to be ensured during the optimization process that the battery does not run out of energy. To achieve this, an edge cost function $\grave{c}_E$, assigning energy consumption costs to edges, is additionally introduced. Again, $\grave{c}_E$ is assumed to be time-dependent for edges which represent road segments:

$$\grave{c}_E(e, t_{arl}) = \text{energy for passing segment } e \text{ at time } t_{arl}$$

Due to the ability of BEVs to recuperate energy, it is possible that the state of charge of a BEV increases while passing a road segment. Hence, $\grave{c}_E(e, t_{arl})$ may return negative values for edges $e \in \vec{E}^\Delta \setminus \vec{E}_{cs}^\Delta$. For charging processes, the energy consumption costs are always negative and equal to the difference between the initial state of charge and the target state of charge:

$$\grave{c}_E\left((v_k^{l\cdot\Delta}, v_k^o), SOC\right) = SOC - l \cdot \Delta \quad (3)$$

$$\grave{c}_E\left((v_k^i, v_k^{l\cdot\Delta}), SOC\right) = 0 \quad (4)$$

To be able to formulate the problem of finding optimal charging strategies as an SPP, it is necessary to have a possibility to represent and pursue the development of the state of charge of the BEV while it is following a recommended charging strategy. For this purpose, an adjusted edge cost function c_E has to be introduced. This function is constructed on the basis of $\grave{c}_E$. Depending on the state of charge SOC when reaching an edge $e \in \vec{E}^\Delta$, c_E is defined as subsequently stated:

$$c_E(e, t, SOC) = \begin{cases} SOC - 1 & \text{if } SOC - \grave{c}_E(e, t) > 1 \\ SOC & \text{if } SOC - \grave{c}_E(e, t) < 0 \\ \grave{c}_E(e, t) & \text{else} \end{cases} \quad (5)$$

Adjustments similar to those described by equation 5 have already been suggested in [8], [9] and [13]. The definition of c_E ensures that for any $e \in \vec{E}^\Delta$, any $t \geq 0$ and any $SOC \in [0, 1]$, the state of charge after passing an edge e remains between 0% and 100%:

$$0 \leq SOC - c_E(e, t, SOC) \leq 1 \quad (6)$$

For a given state of charge at the start of a trip $SOC_S \in [0, 1]$, a given starting time t_S and a given path $P = [v_1, \ldots, v_m]$ (with $m \in \mathbb{N}$), cost function c_E allows computing the state of charge at node v_i (with $i \in \{1, 2, \ldots, m\}$) by reducing SOC_S by the sum of the energy consumption costs assigned to all edges that were passed until node v_i is reached:

$$\text{state of charge at } v_i = SOC_S - c_E(P_{1:i}, t_S, SOC_S). \quad (7)$$

In this context, $P_{1:i}$ represents the subpath of P that consists of its first i nodes, i.e., $P_{1:i} := [v_1, v_2, \ldots, v_i]$. This allows differing between paths representing charging strategies which lead to an empty battery, and other paths. The latter type of paths are denoted as **feasible** paths [4], [19]. Formally, a path

$P = [v_1, \dots, v_m]$ on $\vec{G}^\Delta$ is denoted as feasible if for a given starting time t_S and a given state of charge at the start of the trip SOC_S, the following condition holds:

$$SOC_S - c_E(P_{1:i}, t_S, SOC_S) > 0 \quad \forall i \tag{8}$$

Condition 8 simply states that the state of charge has to be positive whenever a new node along P is reached.

3) A Deterministic Optimization Problem: Let a graph $\vec{G}^\Delta$ and two edge cost functions c_T and c_E be given as described above. Furthermore, let a state of charge at the start $SOC_S \in [0, 1]$, a starting time t_S, a starting node v_s and a destination node v_d in V^Δ be given. Then, the problem of finding optimal charging strategies can be defined as follows:

$$\begin{aligned} \min \quad & c_T(P, t_S, SOC_S) \\ \text{subject to} \quad & P \text{ is a path from } v_a \text{ to } v_d \text{ on } \vec{G}^\Delta \\ & P \text{ is feasible} \end{aligned} \tag{9}$$

This type of SPP is often denoted as a constrained SPP. Please note that the constraint which restricts the optimization to paths that fulfill the feasibility condition is crucial to achieve reliability. Efficiency, however, could also be achieved by alternative objective functions. Minimizing total energy consumption or total energy consumption costs would make some minor adjustments of the described framework necessary, but optimizing these alternative objective functions would still lead to efficient charging strategies, since detours and charging stops cause additional energy consumption and, along with this, additional energy consumption costs. One could also think of further modifications, which ensure a charging behavior that is beneficial for the battery lifespan, e.g. by keeping the state of charge within a certain range. From a modeling perspective, this could be achieved by excluding high target states of charge or by reformulating the feasibility condition in a more restrictive way, but this is out of the scope of this work.

A severe limitation of this formulation of the problem of finding optimal charging strategies is its deterministic nature. If the real energy consumption exceeds the expected energy consumption $\grave{c}_E$–and recent studies indicate that navigation systems in reality often underestimate energy consumption [34]–then a BEV following a correspondingly computed charging strategy may end up with an empty battery. In [22] and [26], a very simple adjustment to solve this limitation is mentioned. There, the feasibility condition is slightly generalized by replacing the zero on the right-hand side of equation 8 by a constant positive number. This lower bound ensures that a certain part of the battery capacity is not taken into account during the optimization process. Instead, this part is considered as a buffer, which can be used to compensate for unexpectedly high energy consumption. As a consequence, reliability may even be achieved in situations in which uncertainty exists. This adjustment of the feasibility condition motivates the following sections.

B. Discussion

When considering the existing literature on charging strategy optimization, most of the papers focus on proposing efficient solution algorithms, which allow computing charging strategies even on huge graphs in reasonable time. Admittedly, this is an important feature and it is absolutely necessary for a potential future application in practice. Though, the necessary efficiency of the optimization algorithms is typically achieved by presuming significant simplifications. Modelling energy and time costs as static values instead of time-dependent variables or allowing only to fully recharge the battery are examples for such simplifications. Another one, on which the focus in the following sections is set, is to ignore the possible existence of uncertainties within the model. One reason for such uncertainties is an imperfect prediction of travel times or energy consumption, which again could be the consequence of individual driving behavior or nonrecurring traffic incidents, such as traffic accidents. Particularly when energy consumption is underestimated, a BEV can easily end up with an empty battery. It is necessary to consider the risks caused by uncertainties. Otherwise, a reliable arrival cannot be ensured and, along with that, range-anxiety remains an unsolved problem. Recalling the literature review, it can be observed that the possible existence of uncertainties is either addressed in a very simple form–by avoiding that the predicted state of charge falls below a positive static bound [15], [22], [26]–or a stochastic problem formulation is derived, which typically suffers from extremely high computation times and significant simplifications [28].

In the following sections, we try to find a compromise between these two extremes. The idea is to extend the simple approaches of [15], [22] and [26] by dynamically adjusting the size of the energy buffer depending on the situation. The resulting problem formulation is still deterministic. Along with this, it is unable to ensure certain arrival probabilities, but it allows handling uncertaints up to some degree. Furthermore, the suggested approach can quite easily be integrated into existing routing algorithms and a critical increase of computation times can be avoided.

III. Charging Strategy Optimization Under Uncertainty

Let a path $P = [v_1, \dots, v_m]$ on $\vec{G}^\Delta$ be given. Furthermore, let ω be a set of not yet specified variables and parameters. P is denoted as **energy secure** if for a given starting time t_S and a given state of charge at the start of the trip SOC_S, the following condition holds:

$$SOC_S - c_E(P_{1:i}, t_S, SOC_S) > SOC_{min}(\omega) \quad \forall i \tag{10}$$

In this context, SOC_{min} is interpreted as a function which returns positive values in dependency of the situation, which again is represented (in an abstract form) by ω. The values which are returned by SOC_{min} are denoted as **minimal energy buffers**. Specific ideas how SOC_{min} and ω could be defined are provided in section III-A.

Replacing the feasibility condition in the formulation of the problem of finding optimal charging strategies by the energy security condition is a very simple adjustment. Nevertheless, it represents a fundamental tool to handle uncertainties - at least if the energy buffer function SOC_{min} is defined

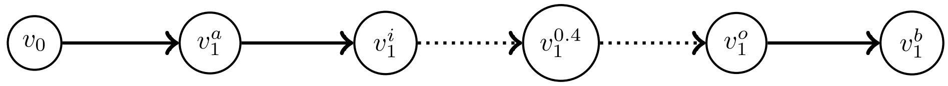

nodes	v_0	v_1^a	v_1^i	$v_1^{0.4}$	v_1^o	v_1^b
SOC [%]	70	40	10	40	40	10
edge leading to node		(v_0, v_1^a)	(v_1^a, v_1^i)	$(v_1^i, v_1^{0.4})$	$(v_1^{0.4}, v_1^o)$	(v_1^o, v_1^b)
$SOC_{min}^{r,z}$ [%] for $z = 1/6$		5	10	0	0	5

Fig. 2. Expected state of charge and the relative energy buffer for $z = 1/6$ along an exemplary path.

appropriately. In this context, "appropriatelly" is interpreted in two different ways: First and foremost, SOC_{min} must return values which are big enough to compensate the difference between experienced and predicted energy consumption. Otherwise, it will happen that the battery of the BEV becomes empty. Second, the minimal energy buffers should not become too big. The bigger the energy buffers, the less charging strategies are able to fulfill the corresponding energy security condition, i.e., the solution space for problem 9 shrinks. Along with this, the recommended charging strategies become more conservative. Higher total travel times are the result and the navigation system will at some point become irrelevant. Furthermore, with an increasing energy buffer size also the probability that no charging strategy can be recommended becomes higher. Consequently, an energy buffer function SOC_{min} should return high buffer values in situations where it is likely that energy consumption is underestimated, and it should provide low values when energy consumption is expected to be predicted quite accurately. It still remains the challenge to define a function SOC_{min} which is able to fulfill these requirements. Some ideas to achieve this are sketched in the next section.

A. Relative Energy Buffer

The concept on which the first type of energy buffer is based is that the longer the distance between two consecutive charging stops is, the higher the energy buffer should become. This can be achieved by increasing the size of the energy buffer with each passed road segment by a certain percentage $z \geq 0$ of the energy that is expected to be necessary for passing this road segment. Whenever a charging process is conducted, the required energy buffer is set back to zero. We refer to this type of energy buffer as **relative energy buffer** and denote the corresponding energy buffer function with $SOC_{min}^{r,z}$ ("r" for "relative"). Let Figure 2 be considered to illustrate $SOC_{min}^{r,z}$ within a small example. A path $P := [v_0, v_1^a, v_1^i, v_1^{0.4}, v_1^o, v_1^b]$ is displayed. This path can be interpreted as a charging strategy which recommends to recharge the battery at charging station 1 up to a state of charge of 40%. To keep the example simple, it is assumed that the energy consumption for passing any edge that represents a road segment (i.e., not the dotted edges) is equal to 30%. Parameter z is set equal to 1/6. The BEV starts with a state of charge of 70%. The table at the bottom of Figure 2 shows the development of the state of charge along path P in the second row. The fourth row depicts the development of the minimal energy buffer according to the energy buffer function $SOC_{min}^{r,z}$ with $z = 1/6$. Note that the minimal energy buffer is set back to 0% during and at the end of the charging process, i.e., at nodes $v_1^{0.4}$ and v_1^o. There are two reasons for doing this: First, the state of charge when leaving a charging station is defined by the path itself. No uncertainty regarding the state of charge exists here, at least if the BEV reaches the charging station. Second, if the minimal state of charge would not be reset to zero, energy buffers would increase further and further along paths. For long distance routes, where several recharging stops are necessary, the energy security condition at the end of the routes would be much more restrictive than at the start–independently of the level of uncertainty in the corresponding situation. This means that even if the charging infrastructure is more dense at the end of the considered route and even if the overall situation at the end could be predicted more precisely than at the start, the energy buffer would increase. This contradicts the purpose of energy buffers to be only as big as necessary. Moreover, the probability that no charging strategy can be recommended due to the energy security condition would increase with the energy that is necessary to follow the whole route.

Please note that the idea of relative energy buffers is quite simple. This has some advantages: Existing algorithms for charging strategy optimization can easily be adjusted in such a way that relative energy buffers are used to compensate for unexpectedly high energy consumption. Furthermore, it is very likely that this adjustment, due to its simplicity, does not have a significant impact on computation times. However, this simplicity causes also limitations: Relative energy buffers only depend on the expected energy costs and do not take the level of uncertainty into account. Furthermore, the approach does in general not allow to represent probabilities. Hence, deriving an appropriate value for z to ensure a certain, minimal arrival probability is in general not possible.

B. Quantile Buffer

Let it be assumed that for each edge e and any arrival time t, not only an expected energy consumption $\grave{c}_E(e, t)$ is available, but a whole probability distribution. Furthermore, let $\grave{c}_E(e, t, \alpha) \in \mathbb{R}_{\geq 0}$ denote the α-quantile of this probability distribution, i.e., α is the probability that the energy consumption for passing edge e at time t is at most equal to $\grave{c}_E(e, t, \alpha)$. Similarly to relative energy buffers, we again start with an energy buffer of 0% and increase it for each passed road segment. However, it is not increased by a certain percentage z of the expected energy consumption, but by the difference between the α-quantile (for some α close to 1.0) and the expected energy consumption. We denote this approach as **quantile buffer** and the corresponding energy buffer function as $SOC_{min}^{q,\alpha}$ ("q" for "quantile"). Quantile buffers can be assumed to be able to fulfill the purpose of energy buffers very well, since the size of this energy buffer particularly increases if it is likely that the predicted or expected, respectively, energy consumption significantly underestimates the real energy consumption. This represents a huge advantage in comparison to relative energy buffers. Still, also this approach suffers from several limitations: Setting α equal to, for example, 99 percent, does not mean that a charging strategy which is based on $SOC_{min}^{q,0.99}$ ensures a 99 percent probability to arrive at the destination. Since each edge is considered separately, it is not trivial to derive overall arrival probabilities from α. Moreover, presuming to know for any edge and any arrival time accurate energy consumption distributions is a very strong and probably unrealistic requirement. Thus, quantile buffers are not part of the simulation study in section V. Nevertheless, they motivate a third approach.

C. Trajectory Buffer

A common approach to predict the energy necessary for passing a road segment e at a time t is to derive, in a first step, a driving trajectory which describes accelerations, decelerations, and driving speeds. In a second step, an energy consumption model $\grave{c}_e$ is applied in order to compute an expected energy consumption value from the trajectory. Instead of computing only one driving trajectory $T^{pre}(e,t)$ ("pre" for "predicted")–and to hope that this trajectory will be equal or, at least, close to the real one–it is suggested to compute an additional set of reasonable driving trajectories $T^{nt}(e,t)$ with $nt \in \{0, 1, .., NT\}$ and $NT \in \mathbb{N}$. These "auxiliary" trajectories lead to additional energy consumption values $\grave{c}_E(e,t,T^{nt}(e,t))$[1]. For each road segment e, the energy buffer is raised by the highest difference between the energy consumption value resulting from the auxiliary trajectories, and the expected energy consumption value $\grave{c}_E(e,t) := \grave{c}_E(e,t,T^{pre}(e,t))$. Similarly as it is done for the relative energy buffer, the new buffer type is reset to zero whenever a charging process is conducted. The corresponding energy buffer is from here on denoted as **trajectory buffer** and the energy buffer function by $SOC_{min}^{t,NT}$ ("t" for "trajectory"). Clearly, the usefulness of the trajectory buffer depends on the way the auxiliary trajectories are generated. If the set of auxiliary trajectories is able to represent the set of all possible future driving trajectories comprehensively, then it is likely that function $SOC_{min}^{t,NT}$ returns values close to $SOC_{min}^{q,\alpha}$ for high values of α. The motivation for the trajectory buffers is to achieve properties similar to those which are expected for the quantile buffers. However, instead of presuming that any relevant energy consumption distribution is available, trajectory buffers can be understood as a construction idea to approximate these probability distributions.

[1]It is written $\grave{c}_E(e,t,T^{nt}(e,t))$ and not $\grave{c}_e(T^{nt}(e,t))$ to emphasize that the energy consumption for passing edge e at time t not only depends on the driving trajectory, but possibly also on further factors, such as the elevation profile of the road segment represented by edge e or the outdoor temperature at time t.

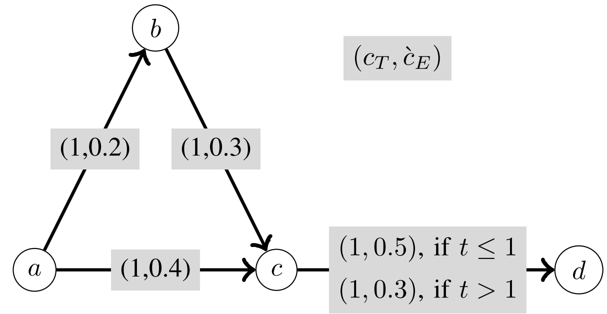

starting	destination	t_S	SOC_S	SOC_{min}
a	d	0	$0.89 = 89\%$	0%

Fig. 3. Edge costs depending on time and the current state of charge.

A limitation, from which all of the suggested energy buffer concepts suffer, is that the uncertainty of travel times is not taken into account. Since energy consumption is assumed to be time-dependent, a possibly postponed arrival at a certain road segment may influence the expected energy consumption, as well as the level of uncertainty that prevails. No details are provided in this paper, but potential adjustments of the problem formulation, which would allow to explicitly consider travel time uncertainty, are discussed in section 5.2 in [4]. The main drawback of the investigated approaches is that computation times would again be raised significantly.

IV. Algorithmic Solution Based on Dijkstra's Algorithm

Problem 9 is, also if the feasibility condition is replaced by the energy security condition, a constrained SPP. This type of problem is proven to be $\mathcal{NP}$-complete [35]. Thus, it can hardly be ensured to compute optimal solutions for this type of problem on big graphs in reasonable time. The situation is actually even worse for problem 9, because Bellman's optimality principle [36] does not hold. In the context of SPPs, i.e., for finding a shortest path between two nodes v_0 and v_K, this principle postulates that any subpath $P^*_{m:n}$ of an optimal path $P^* = [v_0, \ldots, v_K]$ with $0 \leq m < n \leq K$ again is an optimal solution for the problem of finding a shortest path between v_m and v_n. The small graph illustrated in Figure 3 can be found in a very similar form in section 4.1 of [4]. For simplicity, it is assumed that SOC_{min} is constantly equal to 0%. This means that the energy security condition degenerates to the feasibility condition. The graph shows that the Bellman principle does not hold for the described setting: The only feasible, and thus optimal path leading from node a to node d is path $P^* = [a, b, c, d]$. The reason for this is that the energy consumption costs for passing edge (c, d) exceed the energy that is available at node c when following path $\hat{P} = [a, c, d]$ (available energy is 0.49, whereas the energy consumption costs are equal to 0.5). However, the optimal path from node a to node c is $[a, c]$, which is not a subpath of P^*. Clearly, it is counter-intuitive that reaching a certain location later and with a lower state of charge could be beneficial in the end.

Algorithm R: Relative Energy Buffers

Initialization: Create label $L = (0, 0\%, 0, \emptyset, \emptyset, v_a, 1)$ for node v_a. Define set of temporal and of permanent labels $\mathcal{L}_{temp} := \{L\}$ and $\mathcal{L}_{perm} := \emptyset$. Define for each node the highest existing index: $n^{max}(v_a) := 1$, $n^{max}(v) := 0 \quad \forall v \neq v_a$.

While $\mathcal{L}_{temp} \neq \emptyset$ and no label belonging to v_d was added to $\mathcal{L}_{perm}$, do:
    $L^{cur} = (c_T^{cur}, c_E^{cur}, SOC_{min}^{old}, v^{pre}, n^{pre}, v^{cur}, n^{cur})$:= the lexicographically smallest label in $\mathcal{L}_{temp}$.
    Remove L^{cur} from $\mathcal{L}_{temp}$ and add it to $\mathcal{L}_{perm}$.
    For all $v^{new} \in V$ such that $e := (v^{cur}, v^{new}) \in \vec{E}$ do:
        Compute $SOC^{cur} := SOC_S - c_E^{cur}$
        Compute $c_T^{new} := c_T^{cur} + c_T(e, t_S + c_T^{cur}, SOC^{cur})$
        Compute $c_E(e, t_S + c_T^{cur}, SOC^{cur})$ according to equation 5
        Compute $c_E^{new} := c_E^{cur} + c_E(e, t_S + c_T^{cur}, SOC^{cur})$
        If $e \in \vec{E}_{cs}^{\Delta}$, then:
            $SOC_{min}^{new} := 0$
        Else (i.e., e represents a road segment):
            $SOC_{min}^{new} := SOC_{min}^{old} + z \cdot \mid \grave{c}_E(e, t_S + c_T^{cur}) \mid$
        End if.
        Compute $n^{max}(v^{new}) := n^{max}(v^{new}) + 1$
        Compute $n^{new} := n^{max}(v^{new})$
        Create $L^{new} := (c_T^{new}, c_E^{new}, SOC_{min}^{new}, v^{cur}, n^{cur}, v^{new}, n^{new})$
        If L^{new} is not dominated by another label in $\mathcal{L}_{temp}$ or $\mathcal{L}_{perm}$ that belongs to v^{cur} and if $SOC_S - c_E^{new} > SOC_{min}^{new}$, then:
            add L^{new} to $\mathcal{L}_{temp}$ and delete all labels belonging to v^{cur} in $\mathcal{L}_{temp}$ that are dominated by L^{new}.
        End if.
    End for.
End while.
If possible, return a label $\bar{L} \in \mathcal{L}_{perm}$ that belongs to node v_d, otherwise return "No feasible solution found".

Fig. 4. Pseudo-code of the applied algorithm for solving the problem of finding optimal charging strategies.

This intuition is confirmed by the simulation study published in [26]. The study indicates that such situations occur very rarely in the context of charging strategy optimization and have only little influence on the objective function values that can be obtained. As a consequence, the optimization algorithms which are applied in this research to compute charging strategies are designed in such a way that the potential absence of Bellman's optimality principle is not taken into account. Instead, to be able to improve computation times, it is accepted that possibly sub-optimal solutions are computed.

Figure 4 shows the pseudo-code of a dynamic SSP algorithm that includes the idea of relative energy buffers. This algorithm, to which we refer as Algorithm R, can be interpreted as a multicriterial version of Dijkstra's algorithm. It is based on "algorithm 1" from [37]. Besides taking the energy security condition into account, the main difference to the original version of Dijkstra's algorithm is that an extended type of labels is used by Algorithm R. Labels are assigned to nodes of the graph. Each label consists of information about a single path which has been constructed during the route search and which leads from the starting node to the node to which the label is assigned. In Algorithm R, a label L is a 7-tuple:

$$L = \left(c_T^{cur}, c_E^{cur}, SOC_{min}^{cur}, v^{pre}, n^{pre}, v^{cur}, n^{cur}\right) \qquad (11)$$

Values $c_T^{cur} \in \mathbb{R}_{\geq 0}$ and $c_E^{cur} \in [-1, 1]$ describe the cumulated time and energy consumption costs of the path that is described by L. The node to which the label is assigned is denoted by $v^{cur} \in V^{\Delta}$. Several different labels can be assigned during the route search to the same node. The reason for this is explained later on. To be able to differentiate between them, all labels belonging to the same node are numbered consecutively by indices $n^{cur} \in \{1, 2, \ldots\}$. Node $v^{pre} \in V^{\Delta}$ and index $n^{pre} \in \{1, 2, \ldots\}$ identify the preceding label. This information is necessary to reconstruct solution paths. Finally, the value $SOC_{min}^{cur} \in \mathbb{R}_{\geq 0}$ refers to the minimal state of charge that has to be available when reaching node v^{cur}. Here, this value is based on relative energy buffers.

To explain how Algorithm R works, let it be applied to the situation that is illustrated in Figure 3. Let z be equal to 10%. As it is often done in route search algorithms, a set $\mathcal{L}_{temp}$ storing temporal labels, and a set $\mathcal{L}_{perm}$ storing permanent labels are generated in an initial step. Note that Table I shows which labels belong to $\mathcal{L}_{temp}$ and $\mathcal{L}_{perm}$ at the end of the initialization and at the end of each iteration of the while loop. During the initialization, a first temporal label L_a^1 belonging to the starting node v_a is constructed and assigned to $\mathcal{L}_{temp}$. This label actually describes a degenerated path consisting solely of node v_a. The cumulated time and energy consumption costs for

TABLE I
PROCEEDING OF ALGORITHM R FOR THE EXAMPLE FROM FIG. 3

Algorithm R		
Iteration	$\mathcal{L}_{temp}$	$\mathcal{L}_{perm}$
Initialization	$L_a^1 := (0, 0\%, 0\%, \emptyset, \emptyset, a, 1)$	
It. 1	$L_b^1 := (1, 20\%, 2\%, a, 1, b, 1)$, $L_c^1 := (1, 40\%, 4\%, a, 1, c, 1)$	L_a^1
It. 2	L_c^1	L_a^1, L_b^1
It. 3		L_a^1, L_b^1, L_c^1

this path are equal to zero, since no edges have been passed so far. The entries referring to the preceding label remain empty and the minimal energy buffer is set equal to 0%. The values of the last two entries, $v^{cur} = a$ and $n^{cur} = 1$, are a consequence of the fact that this initial label belongs to node v_a and that it is the first label belonging to node v_a. After the initialization, the while-loop is started. Since $\mathcal{L}_{temp}$ is not empty and since no label has yet been added to $\mathcal{L}_{perm}$, both conditions in row 1 are fulfilled. In row 2, label L_a^1 is taken from $\mathcal{L}_{temp}$ and added to $\mathcal{L}_{perm}$, since it is the only label in $\mathcal{L}_{temp}$. If the set of temporal labels contains more than one label, then always the lexicographically smallest label is chosen. In general, a vector $\hat{y} := (\hat{y}_1, \hat{y}_2, \ldots, \hat{y}_n) \in \mathbb{R}^n$ is denoted as **lexicographically** smaller than a vector $\bar{y} := (\bar{y}_1, \bar{y}_2, \ldots, \bar{y}_n) \in \mathbb{R}^n$ if one of the following two conditions hold: Either $\hat{y} = \bar{y}$ or $\hat{y}_j < \bar{y}_j$ with $j := \min\{i : \hat{y}_i \neq \bar{y}_i,\ i \in \{1, \ldots, n\}\}$. This definition is taken from section 5.1 in [38]. For Algorithm R, a label $\hat{L} := (\hat{c}_T, \hat{c}_E, \ldots)$ is called lexicographically smaller than a label $\bar{L} := (\bar{c}_T, \bar{c}_E, \ldots)$ if the accumulated costs $(\hat{c}_T, \hat{c}_E)$ encoded by $\hat{L}$ are lexicographically smaller than the accumulated costs $(\bar{c}_T, \bar{c}_E)$ encoded by $\bar{L}$. In row 5 of Algorithm R, the neighbouring nodes of node v^{cur} are considered, i.e., nodes b and c. In rows 6 to 17, one label for each of these nodes is created. These labels describe paths from the starting node a to the corresponding node. Note that between row 10 and row 14, the minimal energy buffer is adjusted by increasing the original energy buffer at node a, which is equal to 0%, by ten percent of the expected energy consumption. This leads to a minimal energy buffer of 2% for node b. For node c, it leads to 4%. In rows 18 and 19, it is checked if the energy security condition is fulfilled when following these paths. Furthermore, it is checked if the recently constructed label is **domintated** by an already existing label. A label $\hat{L} := (\hat{c}_T, \hat{c}_E, \ldots)$ is dominated by a label $\bar{L} := (\bar{c}_T, \bar{c}_E, \ldots)$ if $\hat{c}_T \geq \bar{c}_T$, $\hat{c}_E \geq \bar{c}_E$ and $\hat{c}_T + \hat{c}_E > \bar{c}_T + \bar{c}_E$. Vice versa, if a label is added to the set of temporal labels, then all existing labels which are dominated by the new one are removed from set $\mathcal{L}_{temp}$. This is done in rows 20 and 21. For the considered situation, two labels are generated during the first iteration of the while-loop, namely L_b^1 encoding path $[a, b]$ and L_c^1 encoding path $[a, c]$. Both labels are also added to the set of temporal labels. During the second iteration, L_b^1 is taken from $\mathcal{L}_{temp}$ and added to $\mathcal{L}_{perm}$. A new label $L_c^2 = (1, 50\%, 5\%, b, 1, c, 2)$ is generated. It encodes the path $[a, b, c]$. This label is dominated by L_c^1 and thus is not added to $\mathcal{L}_{temp}$. During the third and last iteration, L_c^1 is made permanent. The only neighbouring node is d leading to label $L_d^1 = (2, 90\%, 0.9\%, c, 1, d, 1)$. Certainly, the path $[a, c, d]$, which is encoded by L_d^1, does not fulfill the energy security condition. Hence, this label is not added to the set of temporal labels. Consequently, no more labels are part of $\mathcal{L}_{temp}$ when row 1 is reached for the next time. The while-loop ends. Finally, since no label that belongs to node d is part of $\mathcal{L}_{perm}$, no solution has been found by the proposed algorithm.

As already mentioned, the possible absence of Bellman's optimality principle is ignored by Algorithm R. This is also the reason for being unable to finding the optimal path $[a, b, c, d]$. To avoid such a situation, it would be necessary to take also any dominated label into account, i.e., all energy secure paths would be pursued during the route search. This would further increase computation times. Note that computation times for Algorithm R can already increase very quickly with the size of the considered graph. The critical point is that–in contrast to the original version of Dijkstra's algorithm, where only one cost criterion is relevant–many different non-dominated paths may exist between the starting node and any other node. Actually, the number of such non-dominated (or "Pareto optimal") paths can grow exponentially with the number of nodes of the graph [39]. Due to this, any further increase of computation times has to be avoided.

V. SIMULATION STUDY

In this section, the ability of energy buffers to handle uncertainty is tested via simulation. Imperfect predictions of the future development of the prevailing traffic situation are used as source of uncertainty. The simulation study is essential for testing the suggested ideas of energy buffers, because the in fact deterministic optimization problem does not allow deriving a function describing the relation between, for example, the percentage z, which defines the size of the relative energy buffer, and the resulting arrival probability. The following simulation study is intended to provide some first results in this context in order to give an idea of the possibilities and limits of the suggested energy buffer methods.

A. Simulation Environment

The following situation is simulated: A BEV has to pass a 362 kilometers long road corridor without the possibility to use alternative routes. The battery capacity of the BEV is not sufficient to reach the destination, but several charging stations can be found along the road corridor. While passing the road corridor, the BEV experiences changing traffic conditions, which have impact on its driving speed and energy consumption. However, no perfect information about the future development of traffic is available. Instead, only error-prone traffic predictions can be taken into account. At the beginning of the trip, a charging strategy, which is based on these traffic predictions, is provided to the BEV. Whenever the BEV has the possibility to leave the road corridor in order to recharge, it receives an updated charging strategy, which is based on the information that is available at that time (i.e., the BEV's current state of charge, updated traffic predictions, etc.). The purpose of this simulation study is to test and compare different types of energy buffers under different parametrizations.

Certainly, long distance trips are not the primary use case for BEVs. Considering a typical commuting distance of e.g. 40 kilometers would be more relevant from a practical perspective. However, in such a commuting scenario, it is unlikely that several charging stops become necessary. Moreover, the low distance would either lead to only very few charging stations or to a high charging infrastructure density. This would either cause a very small solution space or a quite comfortable situation in which prediction errors could easily be compensated due to the good availability of charging stations. The intention of considering a long-distance use case is to achieve challenging scenarios, which probably reveal the differences between the described energy buffer approaches more clearly.

To simplify explanation, it is differed between setting parameters and scenario parameters. The applied energy buffer function and the considered type of traffic prediction (e.g. historical average driving speeds) form the set of setting parameters. The scenario is defined by the starting time of the virtual trip, the state of charge at the start, parameters describing the charging infrastructure, parameters describing the energy consumption properties of the BEV, the BEV's maximal driving speed, and the simulated outdoor temperature. For each setting, a large set of scenarios is tested. This is done to obtain a comprehensive understanding of how well different energy buffer functions are able to handle the prediction errors coming along with different types of traffic prediction approaches. The assessment of the energy buffer functions is done with respect to two criteria: The average total travel time that a BEV achieves which follows a charging strategy that is based on the considered energy buffer function, and the resutling failure rate. The latter describes how often it happenes during the simulation study that the BEV is unable to reach the destination. This is the case if the BEV runs out of energy during the simulated trip or if at some point during the simulation no charging strategy can be provided which is able to fulfill the energy security condition defined by the considered energy buffer function. If no energy secure charging strategy can be computed at the beginning of the trip, then this type of failure is denoted as pre-trip failure. Any other failure is denoted as an on-trip failure.

Figure 5 visualizes the structure of the simulation study: For each setting, a set of scenarios is tested. After having defined the currently relevant scenario, a first charging strategy is computed for the whole road corridor. This computation is based on Algorithm R and on the available traffic prediction. If a strategy is found that fulfills the currently relevant energy security condition, then it is simulated that the BEV follows the computed charging strategy until the next charging station is reached. If the state of charge of the BEV drops to zero before this next charging station is reached, the scenario is rated as a failure and the next scenario is tested. The same happens if no energy secure charging strategy can be found. Otherwise, i.e., if the next charging station is reached, an updated charging strategy computation takes place. Again, it is checked whether an energy secure strategy can be found and whether the BEV runs out of energy until the next charging station is reached. This procedure is continued until the destination is reached or the BEV fails to pass the scenario.

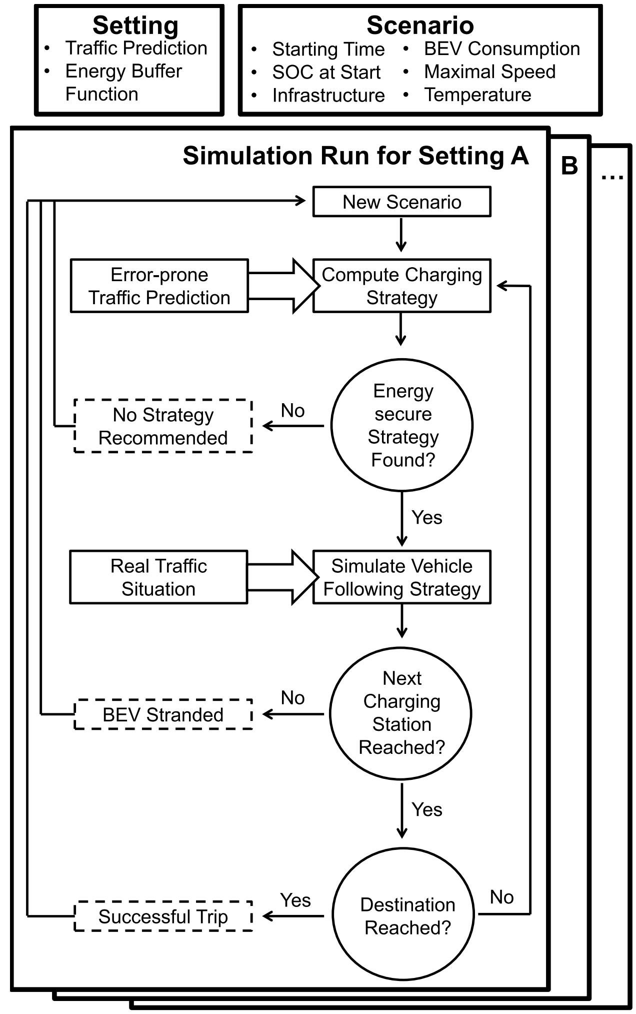

Fig. 5. Structure of simulation study.

1) Simulated Traffic Situation: The traffic situation which the BEV experiences during the simulation is described by a spatio-temporal speed function V_{GT} ("GT" for "ground truth"). This function returns a speed value in dependency of time and space. Let an interval $X = [x_{min}, x_{max}] \subset \mathbb{R}_{\geq 0}$ describe the road corridor that needs to be passed and let the interval $T = [t_{min}, t_{max}] \subset \mathbb{R}_{\geq 0}$ denote the time period during which the simulated trips are done. Function V_{GT} can be introduced as follows:

$$V_{GT} : X \times T \longrightarrow \mathbb{R}_{\geq 0}$$
$$V_{GT}(x, t) = \text{speed at time } t \text{ and location } x$$

To achieve reasonable results, i.e., to ensure that V_{GT} shows realistic properties, it is based on inductive loop detector data. As described before, a several hundred kilometer long road corridor is considered. This ensures that the simulated BEV has to recharge its battery several times before reaching the destination. For the described research, only a limited amount of detector data, kindly provided by the South-Bavarian Freeway Authority, is available. Unfortunately, the data does not cover a several hundred kilometer long road corridor. Thus,

TABLE II
INFORMATION ON TEST SITES

corridor & direction	length [km]	number of lanes	start of corridor - end of corridor	number of detectors	number of days
A9 northbound	39	3-4	interchange Munich north - exit ramp Geisenhausen	27	4
A9 southbound	26	3-4	exit ramp Allershausen - interchange Munich north	22	6
A99 clockwise	33	2-5	exit ramp Ludwigsburg - exit ramp Hohenbrunn	26	4
A99 counter-clockwise	35	2-5	exit ramp Ottobrunn - junction Munich - Feldmoching	29	8

inductive loop detector data from several road corridors is concatenated in such a way that a single, 362 kilometer long road corridor results. Table II provides some general information about these corridors. The data has been recorded on two German freeways, the A9 and the A99. The first one starts in Munich and connects it with Nürnberg and later on with Berlin. The second freeway forms almost a full circle around Munich. The inductive loop detector data is given at one-minute resolution and contains several types of traffic information. Here, only recorded driving speeds and the time at which the data was recorded are relevant. The data is aggregated over all lanes, i.e., no lane specific information is considered. The distances between two consecutive detectors range between a few hundred meters and more than three kilometers.

To get from the inductive loop detector data to the spatio-temporal speed function V_{GT}, the traffic state reconstruction approach which is described in [40] is applied. This method is an adjusted version of the widely known "adaptive smoothing method" (ASM), which was initially proposed by Treiber [41]. The ASM is an interpolation scheme which takes the typical propagation speeds of information in freeway traffic into account. The interpolation makes it possible to derive a continous spatio-temporal speed function from detector data which is only punctually available. The adjustment in [40] reduces the computational effort for applying the ASM and, at the same time, keeps the quality of the reconstruction high.

The construction of function V_{GT} is finally done as follows: First, for each of the four road corridors and for each day for which data is available, a separate traffic state reconstructions is made. The last column in Table II shows the number of days during which inductive loop detector data from the corresponding road corridor has been gathered. This means that in total 22 $(= 4+6+4+8)$ traffic state reconstructions–each describing a single day for one of the four road corridors–are available. In a second step, these 22 single speed functions are arranged on the spatio-temporal plane in such a way that 362 kilometers and a two days period are covered. The contour plot of the resulting function V_{GT} is shown in Figure 6. The small red areas indicate congestion, whereas the green areas refer to situations during which high speeds have been realized. Note that V_{GT} covers a three days period and that the last day is a copy of the first day. Furthermore, it has to be mentioned that–though the traffic state reconstructions that are done for each day and each road corridor should represent a realistic picture of the corresponding traffic situation–the

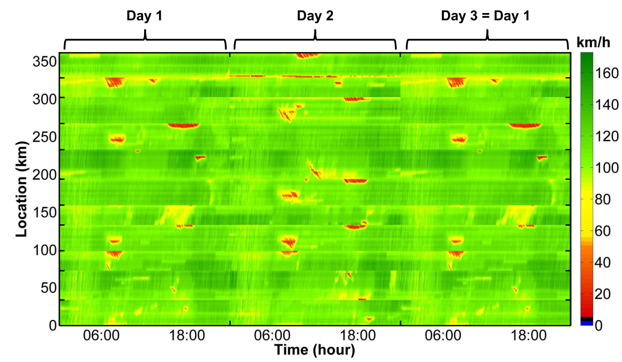

Fig. 6. Function V_{GT} which is used in simulation.

concatenation of these spatio-temporal speed functions leads to unrealistic phenomena. Discontinuities occur particularly at the spatial borders between the separately generated traffic state reconstructions, i.e., presumed driving speeds change in some situations drastically from one moment to the other. Later on, it is described why it can be assumed that these discontinuities are not critical for the simulation study.

2) Simulation of Energy Consumption and Travel Times: The generated traffic situation V_{GT} is used to derive travel times and energy consumption values for the BEV. This is done in two steps: First, driving trajectories are derived from the spatio-temporal speed function V_{GT}. If at a time t_S the BEV begins passing a certain part of the road corridor, which is represented by an edge e, while facing traffic conditions described by V_{GT}, then a unique driving trajectory can be derived by solving the ordinary differential equation

$$\frac{dx}{dt} = V_{GT}(x(t), t) \tag{12}$$

with initial condition $x(t_S) =$ start of e [42]. The computation is terminated as soon as the end of e is reached. Let this time be denoted as $t_{end}(e)$. The location of the BEV x is interpreted in equation 12 as a function of time. The time necessary for passing edge e results directly from the function $x^*(t)$ which solves the problem described in equation 12. The corresponding energy consumption is derived in a second step. For this purpose, a simple energy consumption model, which consists of two components, is applied to the derived driving trajectories. Its first component E_{Prim} assigns instantaneous energy consumption values (given in watt) to driving speeds. It represents the BEV's primary energy consumption, i.e., the energy necessary for propulsion, and can be interpreted as a real-valued function:

$$E_{Prim} : \mathbb{R}_{\geq 0} \longrightarrow \mathbb{R}_{\geq 0} \tag{13}$$

This component is based on real consumption data from almost eleven thousand trips with BEVs. The trips were made by 23 privately owned BMW i3 in 2015 and 2016. The recording of the energy consumption data took place in the project "PREMIUM", which was funded by the (German) Federal Ministry for the Environment, Nature Conservation, Building and Nuclear Safety. The BEVs were equipped with sensors for measuring driving speeds and the energy consumption which is necessary for propulsion. The data was recorded with a frequency of ten hertz. Unfortunately, no information about the geographical position of the BEVs or about the road stepness was recorded. For the first component of the energy consumption model, simply the average instantaneous energy consumption in dependency of the driving speeds is computed based on the available data. Due to a nondisclosure agreement with BMW, the authors are not allowed to provide here any detailed information. Nevertheless, it can be stated that the resulting primary energy consumption per kilometer shows the shape of an asymmetric parabola, i.e., the consumption per kilometer is high for low and for high speeds.

The second component E_{Sec} of the applied energy consumption model represents the BEV's secondary energy consumption, i.e., all energy that is not used for propulsion. This component was kindly provided by BMW within the project "DC-Ladestation am Olympiapark", which was funded by the (German) Federal Ministry of Transport and Digital Infrastructure. It desribes the secondary energy consumption of a BMW i3 in dependency of the outdoor temperature. Note that the secondary energy consumption is typically dominated by the consumption necessary for operating the air conditioning, which strongly depends on the outdoor temperature. Again, no details can be provided due to a nondisclosure agreement. Still it can be said that high temperatures (due to cooling) and low temperatures (due to heating) cause increased energy consumption of the air conditioning and, along with that, an increased secondary energy consumption. Particularly temperatures below the freezing point lead to a significant uplift.

In total, the energy consumption $\grave{c}_E(e, t_S)$ for passing edge e at time t_S, given a traffic situation described by V_{GT}, can then be computed as follows:

$$\int_{t_S}^{t_{end}(e)} E_{Prim}\left(V_{GT}\left(x^*(t), t\right)\right) + E_{Sec}\left(Tp\left(x^*(t), t\right)\right) dt \tag{14}$$

Function $Tp \in \mathbb{R}$ describes here the outdoor temperature in dependency of location and time. Furthermore, it has to be mentioned that this energy consumption model suffers from some limitations. Road steepness, for example, is not taken into account and due to the way E_{Prim} is derived, accelerations and decelerations are not considered. Fortunately, the latter ensures that the existance of discontinuities in V_{GT} does not lead to unreasonable energy consumption values.

3) Types of Error-Prone Traffic Predictions: In total, five different types of traffic predictions are used during the simulation study as a basis for the charging strategy computation. The first type is a perfect traffic prediction $V_{Perf}^{t_B}$. The variable $t_B \in \mathbb{R}_{\geq 0}$ describes the time at which the prediction is requested. For prediction $V_{Perf}^{t_B}$, this variable is not relevant, since $V_{Perf}^{t_B}$ always mirrors the real traffic situation V_{GT} perfectly:

$$V_{Perf}^{t_B}(x, t) = V_{GT}(x, t). \tag{15}$$

Please note that being able to predict future traffic perfectly is not realistic. Considering this type of traffic prediction is motivated by academic considerations. The second type of applied traffic prediction is a so-called instantaneous traffic prediction $V_{Inst}^{t_B}$:

$$V_{Inst}^{t_B}(x, t) := V_{GT}(x, t_B) \quad \text{for } t \geq t_B. \tag{16}$$

Function $V_{Inst}^{t_B}$ returns for all future times the currently prevailing traffic conditions. This leads typically to good results for short-term predictions. The third type of traffic prediction is denoted by $V_{ff}^{t_B}$. "ff" is an abbreviation for "free flow". This function can be interpreted as a situation in which no information about future driving speeds is available and thus simply free flow is presumed. Note that during the simulation, free flow means that the BEV drives with a maximal driving speed V_{Max} which is defined by the scenario that is currently tested:

$$V_{ff}^{t_B}(x, t) := V_{Max}. \tag{17}$$

The forth type makes use of historical speed averages $V_{Hist}^{t_B}$. The corresponding speed values for the four considered freeway corridors, on which V_{GT} is based, are provided by TomTom. They show the historical average driving speeds in dependency of the location, the time of the day, and the day of the week. The last type of traffic prediction is denoted by $V_{Pha}^{t_B}$ ("Pha" stands for "phantom congestion"). If t is part of the first/second day, it is defined as follows:

$$V_{Pha}^{t_B}(x, t) := \min\{V_{GT}(x, t), V_{GT}(x, t + 1 \text{ day})\} \tag{18}$$

Otherwise, $V_{Pha}^{t_B}(x, t)$ results as subsequently stated:

$$V_{Pha}^{t_B}(x, t) := \min\{V_{GT}(x, t), V_{GT}(x, t - 1 \text{ day})\} \tag{19}$$

Recall that V_{GT} represents a three days period, where the speeds belonging to the first day are copied and additionally used for the third day. Prediction $V_{Pha}^{t_B}$ returns for any (x, t) either the real driving speed $V_{GT}(x, t)$, or, if it is lower, the driving speed that is returned by V_{GT} for one of the neighbouring days for the corresponding location and time of the day. Thus, function $V_{Pha}^{t_B}$ tends to underestimate real driving speeds. The motivation for the construction of $V_{Pha}^{t_B}$ is to understand the impact of incorrectly predicted traffic congestion on the quality of the charging strategies. This can be interpreted as a counterpart to the free flow assumption done by $V_{ff}^{t_B}$, where driving speeds are systematically overestimated.

4) Scenario Parameters: For each setting, consisting of an energy buffer function and a prediction type, a set of 1440 different scenarios is tested. The sequence of scenarios that is tested remains the same for each setting. To get different scenarios, each of the six aforementioned types of scenario parameters is changed with each scenario. The state of charge at the start is randomly chosen between

0% to 100%. The same holds for outdoor temperature, but these values range from −10°C and +35°C. For simplicity, temperature is assumed to be constant over time and space. The maximal driving speed, which can be understood as the highest speed the BEV is able to drive, is equal to 90, 100, 110, 120 or 130 kilometers per hour. Starting times are chosen in steps of two minutes, starting at 00:00 in the morning of the first day and ending at 23:58 at the end of the second day for which V_{GT} is constructed. Moreover, it is iterated over one of four different charging infrastructure scenarios. These scenarios assume the availability of 7, 9, 11 or 13 charging stations along the 362 kilometers long road corridor. Note that there is always a charging station located at the start of the road corridor, i.e., the BEV can be recharged before starting the trip. Finally, three different types of BEVs are considered. They differ in terms of energy consumption and recharging behavior. The energy consumption model that has been described in section V-A.2 refers to the first type of BEV. Furthermore, it is assumed that the battery of this BEV has the same capacity as the first generation of the BMW i3, i.e., 67,680,000 joules [43]. Also the charging behavior is assumed to be similar to the charging behavior of a BMW i3: Up to a state of charge of 80%, it is assumed that 22.5 seconds are necessary for increasing the state of charge by 1%. The consequence is that the battery can be recharged from 0% to 80% in exactly 30 minutes. For states of charge above 80%, the charging duration for each percent increases to 90 seconds. Hence, recharging from 80% to 100% lasts another 30 minutes. For the second type of BEV, the battery capacity and the recharging times are reduced by 20%. Additionally, the primary energy consumption model is adjusted in such a way that the second type of BEV consumes more energy for high speeds and less energy for very low speeds. The secondary energy consumption is also reduced. For the third type of BEV, the battery capacity and the charging durations are increased by 40% in comparison to the first type of BEV. The primary (particularly for low driving speeds) and the secondary energy consumption are raised.

B. Simulation Results for Relative Energy Buffers

In this section, the results of the simulation study for relative energy buffers are discussed. Function $SOC_{min}^{r,z}$ with $z \in \{0.0\%, 2.5\%, 5\%, 10\%, 20\%, 30\%, 40\%\}$ is applied to define whether or not a certain charging strategy is considered to be energy secure. The higher the value of z is, the more restrictive the energy security condition becomes. To explain the analysis results, let the upper part of Figure 7 be considered. It shows the results when using traffic prediction $V_{Perf}^{t_B}$ for the derivation of charging strategies, i.e., in this situation, no prediction errors exist. Average total travel times, i.e., the sum of average driving and average charging times, can be found on the x-axis and the number of failures on the y-axis. Each of the displayed triangles describes the outcome for one specific setting. The numbers placed near the triangles show the value (in percent) of parameter z which belongs to the corresponding setting. Comment 1 in Figure 7 exemplarily explains how the rightmost triangle in the upper part of Figure 7 can

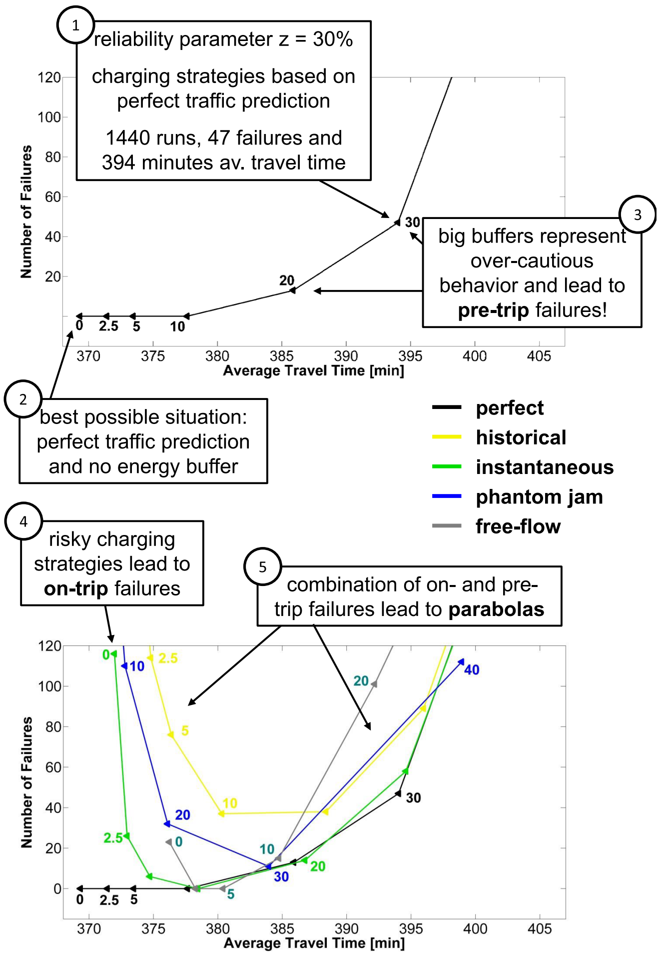

Fig. 7. Results of the simulation runs when applying relative energy buffer functions.

be interpreted: This triangle results when applying function $SOC_{min}^{r,z}$ with $z = 30\%$ and using perfect traffic predictions as input for the charging strategy computation. During the 1440 conducted simulation runs, 47 failures occur and the remaining 1393 scenarios lead to an average total travel time of about 394 minutes. The leftmost triangle shows that no failures occur and, at the same time, that the average total travel time can be reduced down to 369 minutes if parameter z is set equal to 0%. The latter actually means that no energy buffer is applied at all. This would be critical if the applied traffic prediction was error-prone. However, function $V_{Perf}^{t_B}$ is used here. Thus, no uncertainty exists at all for this setting and applying no buffer is the best that can be done (see comment 2).

With increasing parameter z, the number of charging strategies which are able to fulfill the corresponding energy security condition becomes smaller. Less solution possibilities reduce the optimization potential. The consequence is, as can be seen in the upper part of Figure 7, that the average total travel times increase. If z becomes big enough, the number of energy secure charging strategies is reduced down to zero for some of the simulated scenarios. Consequently, pre-trip errors occur, i.e., no charging strategy can be recommended at the beginning of the trip. In the simulation study, this is the case for z equal to 20% or higher. This can be interpreted as over-cautious behavior (see comment 3). Clearly, big energy buffers cause pre-trip failures also for error-prone types of traffic predictions. However, in contrast to the case of perfect traffic predictions, uncertainty exists for these settings. Thus, being too optimistic can lead to situations in which the battery runs out of energy during the trip. The consequences are on-trip failures. The lower part of Figure 7 displays the simulation results also for the aforementioned error-prone types of traffic predictions. Particularly for the green (instantaneous driving speeds), the blue (phantom jams) and the yellow curve (historical speed averages), it can be observed that low values for z cause a lot of failures (see comment 4). Note that due to the combination of on-trip failures for small buffers and pre-trip failures for big buffers, and due to the fact that average total travel times grow with the size of the energy buffer, the curves belonging to error-prone traffic predictions show a shape similar to a parabola (see comment 5). For the gray curve, belonging to traffic prediction $V_{ff}^{t_B}$, it seems that the left branch of the parabola is cut off only shortly left of the vertex. This is a consequence of ending up with only 23 on-trip failures even though no energy buffer was used at all. Presuming always free flow traffic conditions leads to a systematic over-estimation of driving speeds. Since the applied primary energy consumption model assigns high energy consumption values to high driving speeds, also energy consumption is systematically over-estimated. The only exceptions are very few situations in which the simulated BEV experiences driving speeds that remain extremely low for several kilometers. For extreme low driving speeds, the energy consumption per kilometer can be higher than when driving with maximal speed. Hence, it can only happen in these comparably rare situations that the experienced energy consumption exceeds the energy consumption prediction based on $V_{ff}^{t_B}$. This means that traffic prediction $V_{ff}^{t_B}$ implicitely leads to the same effect as when applying big energy buffers. The opposite can be observed for $V_{Pha}^{t_B}$, where driving speeds are systematically underestimated: In many situations, the systematic underestimation of driving speeds causes a systematic underestimation of energy consumption, which again eventually leads to on-trip failures even for moderate values of z. The underestimation of maximum driving speeds in near free-flow situations represents also the main failure reason for functions $V_{Inst}^{t_B}$ and $V_{Hist}^{t_B}$. This observation is particularly interesting, since the driver of a BEV would be able to reduce the driving speed in such situations. This would reduce energy consumption and the next charging station may still be reached. If failures are caused by an unexpected traffic jam, then the driver cannot simply increase the driving speed. This lack of a reaction possibility makes failures caused by unexpected traffic congestion, though this occurred less often within the simulation study, more critical from a practical perspective.

If this type of simulation study was used to identify for a given traffic prediction scheme the value of z that leads to the best charging strategies, then the parabolic shape of the described curves would suggest to choose low values for z rather than being too conservative. The reason for this is that the results for any triangle belonging to the right branch of a parabola are dominated by the results belonging to the vertex of the parabola, since the vertex necessarily indicates a lower average total travel time and a lower failure rate. Values of z belonging to the left branch of the parabola, on the other hand, allow improving travel times at the cost of additional failures. Important is in this context that if using the curves displayed in Figure 7 in order to determine a good value for z, then one implicitly assumes that on-trip failures are not worse than pre-trip failures. This may not represent the opinion of the driver of a BEV, who may accept to sometimes use a different transportation mode if no energy secure charging strategy can be computed, but who probably is not willing to risk running out of energy during a trip. A possible adjustment to take the driver's preferences into account is to weight pre-trip failures differently.

The main purpose of the conducted simulation study is to analyze the ability of the concept of energy buffers to handle uncertainties. If the results in the lower part of Figure 7 are taken into account, then it can be stated that even the simple idea of relative energy buffers is able to achieve quite low failure rates for most of the tested traffic prediction approaches. For $V_{Perf}^{t_B}$, $V_{ff}^{t_B}$ and $V_{Inst}^{t_B}$, the appearance of failures can completely be avoided. The main problem is $V_{Hist}^{t_B}$. For this prediction type, the number of failures is at least equal to 37, leading to a minimal failure rate of $37/1440 = 2.6\%$ for $z = 10\%$. The question is whether a different type of energy buffer is able to improve the results.

C. Comparison Between Relative and Trajectory Buffers

In the simulation study, also trajectory buffers are tested for some of the described traffic prediction approaches. The pseudo-code of the corresponding SPP algorithm is not provided, but its implementation follows the ideas described in section IV. The energy consumption prediction $\grave{c}_E(e, t, T^{pre}(e, t))$ (see section III-C) during the simulation runs is based on a trajectory T^{pre} that is derived from the applied traffic prediction scheme. Since it is not important which type of traffic prediction approach is applied, let this prediction for the moment be denoted by $V_{Pred}^{t_B} \in \{V_{Perf}^{t_B}, V_{ff}^{t_B}, V_{Inst}^{t_B}, V_{Hist}^{t_B}, V_{Pha}^{t_B}\}$. Driving trajectory T^{pre} is then received by solving differential equation 12 while replacing V_{GT} by $V_{Pred}^{t_B}$ on the right-hand side. The approach for constructing auxiliary trajectories T^{nt} is kept simple. A parameter $f \in [0, 1]$ is introduced and the auxiliary trajectories T^{nt} are derived by replacing V_{GT} in equation 12 by the spatio-temporal speed function $V_{nt}^{t_B, f}$, which assigns to each point (x, t) the following value in dependency of $nt \in \{0, 1, \ldots, NT\}$:

$$\left(1 - \frac{nt}{NT}\right) \cdot (1 - f) \cdot V_{Pred}^{t_B}(x, t) + \frac{nt}{NT} \cdot (1 + f) \cdot V_{Pred}^{t_B}(x, t)$$

This idea for generating a set of auxiliary trajectories is also illustrated in Figure 8. The auxiliary trajectories are intended to comprehensively cover the spatio-temporal area that lies between the trajectories that are derived from functions $(1 - f) \cdot V_{Pred}^{t_B}$ and $(1 + f) \cdot V_{Pred}^{t_B}$. In order to keep the computational effort for the simulation runs reasonably low, only two auxiliary trajectories are computed to derive the energy buffer function $SOC_{min}^{t,NT}$, i.e., parameter NT is set

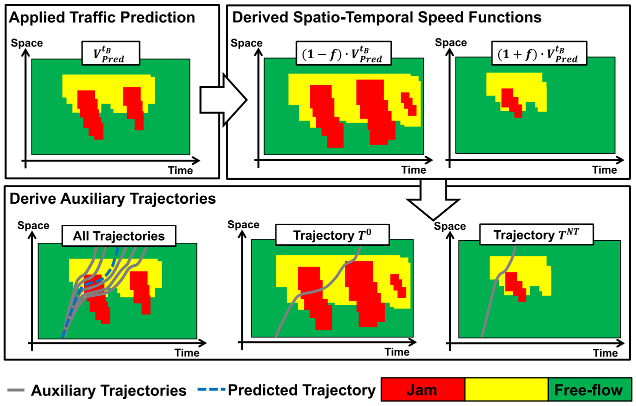

Fig. 8. Generation of a trajectory set on the basis of speed bound functions.

equal to 1. Please note that $SOC_{min}^{t,NT}$ is corrected to zero if it would return a negative value.

The trajectory buffers have been tested for the traffic prediction functions $V_{Perf}^{t_B}$, $V_{Hist}^{t_B}$ and $V_{Inst}^{t_B}$, and for parameter $f \in \{0.05, 0.1, 0.2, 0.5, 0.7\}$. Note that $f = 0$ is not tested, since this would lead to the same values as $z = 0\%$. The results of the simulation runs can be found in Figure 9. Stars mark the results achieved by applying trajectory buffers, triangles refer again to relative energy buffers. The numbers that can be found in the graphs of Figure 9 either describe the values of z or f. To simplify differentiation, a %-sign is added whenever a number refers to z. Let at first Figure 9(a) be considered, where the average total travel time and failure numbers are shown that result when computing charging strategies based on perfect traffic predictions. It can be observed that both displayed curves behave very similarly: With increasing the value of the applied parameter (z or f), the average total travel time increases and at some point, failures occur– even though no uncertainty exists. For the applied trajectory buffer, this observation shows that the size of the energy buffers increases when raising the values of f. The reason for this is that higher values of f cause the two generated auxiliary trajectories to deviate more significantly from the predicted driving trajectory. This tends to lead to higher differences between the resulting energy consumption values, which again increases the size of the energy buffer. However, this is not always the case, i.e., increasing f sometimes reduces the size of the energy buffer. The consequence is that higher values of f may even decrease failure rates. This rarely occurring phenomenon causes that the curve in Figure 9(c), which belongs to trajectory buffers, is not convex.

When considering the graphs in Figure 9, then both energy buffer approaches show advantages in different situations. In Figure 9(a), the results that can be achieved do not differ much. In Figure 9(b), when relying on predictions based on historical average driving speeds, it can be seen that the trajectory buffers outperform relative energy buffers, as the number of failures can be reduced from 37 to 6. This is a very important observation, because $V_{Hist}^{t_B}$ is the type of traffic prediction for which the worst failure rates occurred in Figure 7.

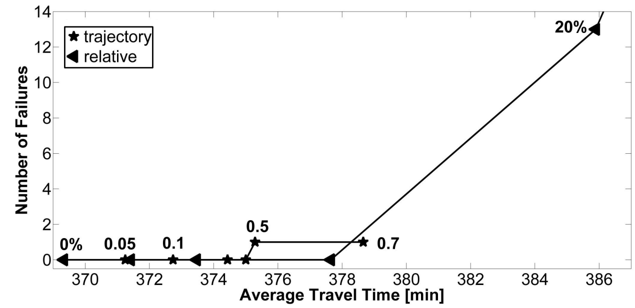

(a) Assumption of perfect traffic prediction.

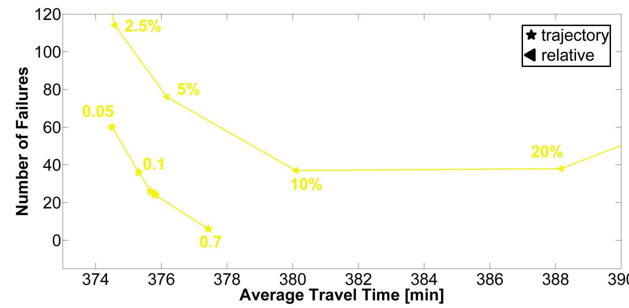

(b) Applying historical speed averages.

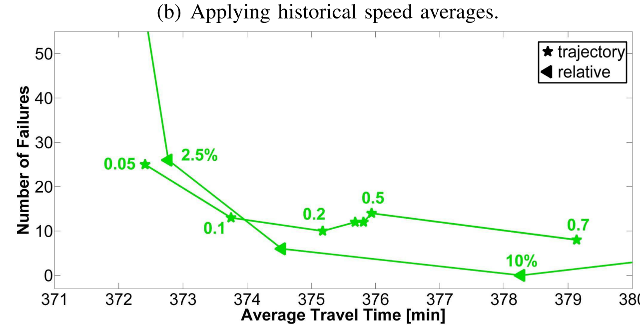

(c) Applying instantaneous travel time predictions.

Fig. 9. Comparison of relative and trajectory buffer.

On the contrary, relative energy buffers make it possible to completely avoid failures when making use of instantaneous traffic predictions. For trajectory buffers, at least for the tested values of f, this is not the case as can be seen in Figure 9(c). In conclusion, these first simulation results indicate that the concept of energy buffers could be very well suited for handling uncertainties when computing charging strategies. Interesting in this context is that the two applied approaches, even though their design is very simple, allow keeping failure rates quite low. Still, an on-trip failure rate of $6/1440 = 0.4\%$, as it can be observed for the conducted simulation runs when using prediction $V_{Hist}^{t_B}$ to derive charging strategies, is not sufficient for a practical application. It would mean that for about one of 250 trips, the BEV would not reach its destination. On the other hand, by adjusting values z and f, on-trip failures can be traded against pre-trip failures and increased travel times. The simulation results in Figures 7 and 9 indicate that the impact of conservatively chosen parameters z and f on travel times is very limited. Moreover, the existence of a few pre-trip failures might be acceptable–also in practice. Thus, using high values for z and f may already lead to good results in reality.

TABLE III
NOMENCLATURE

Δ	parameter defining difference between consecutive target states of charge
$\vec{G}^{\Delta} = (V^{\Delta}, \vec{E}^{\Delta})$	graph representing the road network and charging possibilities
$\vec{E}^{\Delta}_{cs}$	edges representing parts of charging processes
SOC	state of charge
c_T	cost function assigning time costs to edges
$\grave{c}_E$	cost function assigning energy consumption costs/gains to edges
c_E	adjusted version of $\grave{c}_E$ ensuring that the state of charge remains between 0 and 1
$P_{m:n}$	subpath of path P from its m-th to its n-th node
$SOC^{r,z}_{min}$	relative energy buffer function with parameter z
$SOC^{q,\alpha}_{min}$	quantile buffer function with parameter α
$SOC^{t,NT}_{min}$	trajectory buffer function with parameter NT
T^{pre}	predicted driving trajectory
T^{nt}	nt-th auxiliary driving trajectory
L^i_a	the i-th label belonging to node a
$\mathcal{L}_{temp}$	set of temporary lables
$\mathcal{L}_{perm}$	set of permanent lables
E_{Prim}	function returning the BEV's primary energy consumption in dependency of driving speed
E_{Sec}	function returning secondary energy consumption in dependency of outdoor temperature
$V_{GT}(x,t)$	ground truth speed function representing actual driving speeds
$V^{t_B}_{Perf}$	traffic prediction function requested at time t_B providing perfect information
$V^{t_B}_{Inst}$	traffic prediction returning instantaneous driving speeds
$V^{t_B}_{ff}$	free-flow traffic prediction
$V^{t_B}_{Hist}$	traffic prediction providing historical speed averages
$V^{t_B}_{Pha}$	traffic prediction reporting phantom congestion

VI. CONCLUSION

There are two main contributions of the described research: First, an existing deterministic model for the optimizing of charging strategies for BEVs is extended in such a way that uncertainties can be handled. To achieve this, the feasibility condition, which is typically used if navigation applications for BEVs are considered, was generalized in section III by introducing the idea of situation-dependent energy buffers. This generic adjustment was then concretized in sections III-A to III-C by proposing three different approaches that dynamically adjusts the size of the energy buffer in dependency of the situation. These adjustments are intended to compensate for uncertainties of the available energy consumption prediction. In section IV, a specific algorithmic implementation is exemplarily described for one of these approaches. This algorithm represents the second main contribution, since it can be understood as a template for including energy buffers into existing routing algorithms for BEVs. By providing such exemplary pseudo-code, the authors hope to facilitate shifting the focus in this area of research from further improving computational speed to ensuring a more reliable arrival at the destination. Please note that, despite the fact that uncertainties represent a stochastic phenomenon, both algorithms still are part of a fully deterministic model. Stochastic approaches can be expected to increase computational effort significantly. Moreover, for the described setting, they would need a lot of information, such as a time-dependent probability distribution of energy consumption for all relevant road segments. The simplicity of the described algorithms, however, makes it hard to analytically compute arrival probabilities. Thus, two of the suggested energy buffer concepts were afterwards tested within a simulation study in order to get a first idea of the ability of the proposed concept to handle the existence of uncertainty. The results of the simulation study were promising, since the failure probabilities could be kept in general significantly below one percent. However, it has to be mentioned that the conducted simulation runs suffer from several limitations, such as considering only one source of uncertainty, namely traffic prediction errors. Furthermore, the described simulation study covers solely a limited range of situations and it is based on loads of assumptions. It is not very likely that all situations that could occur in reality are represented adequately and comprehensively. Further studies, in which different assumptions are made and different sources of uncertainty are considered, are necessary to get a more comprehensive understanding of the possibilities and limitations of the concept of energy buffers.

ACKNOWLEDGMENT

The authors want to thank the South-Bavarian Freeway Authority for providing the inductive loop detector data.

REFERENCES

[1] World Health Organization. *7 Million Premature Deaths Annually Linked to Air Pollution*. Accessed: Nov. 11, 2017. [Online]. Available: http://www.who.int/mediacentre/news/releases/2014/air-pollution/en/

[2] Nationale Plattform Elektromobilität (NPE). (2014). *Fortschrittsbericht 2014–Bilanz der Marktvorbereitung*. Accessed: Jun. 27, 2016. [Online]. Available: http://www.din.de/blob/67180/c6df394edbef17083c6c845e50c82275/npe-f-bericht14-data.pdf

[3] N. Rauh, T. Franke, and J. F. Krems, "User experience with electric vehicles while driving in a critical range situation–a qualitative approach," *IET Intelligent Transport Systems*, vol. 9, no. 7, pp. 734–739, 2015.

[4] G. Huber, "Optimization of charging strategies under the consideration of error-prone traffic information," Ph.D. dissertation, Dept. Civil Eng., Univ. Federal Armed Forces Munich, Neubiberg, Germany, 2017.

[5] S. Kluge *et al.*, "On the computation of the energy-optimal route dependent on the traffic load in Ingolstadt," *Transp. Res. C, Emerg. Technol.*, vol. 36, pp. 97–115, Nov. 2013.

[6] M. W. Levin, M. Duell, and S. T. Waller, "The effect of road elevation on network wide vehicle energy consumption and ecorouting," *Transp. Res. Rec. J. Transp. Res. Board*, vol. 2427, pp. 26–33, 2015.

[7] B. Hesse, "Einfluss verschiedener Nebenverbraucher auf Elektrofahrzeuge," in *Zukünftige Entwicklungen in der Mobilität: Betriebswirtschaftliche und Technische Aspekte*. Wiesbaden, Germany: Springer, 2012, pp. 91–104.

[8] J. Eisner, S. Funke, and S. Storandt, "Optimal route planning for electric vehicles in large networks," *Proc. 25th AAAI Conf. Artif. Intell.*, 2011, pp. 1108–1113.

[9] T. Jurik *et al.*, "Energy optimal real-time navigation system: Application to a hybrid electrical vehicle," in *Proc. 16th Int. IEEE Conf. Intell. Transp. Syst. (ITSC)*, Oct. 2013, pp. 1947–1952.

[10] E. W. Dijkstra, "A note on two problems in connexion with graphs," *Numerische Math.*, vol. 1, no. 1, pp. 269–271, Dec. 1959.

[11] R. W. Floyd, "Algorithm 97: Shortest path," *Commun. ACM*, vol. 5, no. 6, p. 345, Jun. 1962.

[12] D. B. Johnson, "Efficient algorithms for shortest paths in sparse networks," *J. ACM*, vol. 24, no. 1, pp. 1–13, 1977.

[13] M. Baum, J. Dibbelt, T. Pajor, and D. Wagner, "Energy-optimal routes for electric vehicles," in *Proc. 21st ACM SIGSPATIAL Int. Conf. Adv. Geographic Inf. Syst. (SIGSPATIAL)*, 2013, pp. 54–63.

[14] T. Ichimori, H. Ishii, and T. Nishida, "Routing a vehicle with the limitation of fuel," *J. Oper. Res. Soc. Jpn.*, vol. 24, no. 3, pp. 277–281, 1981.

[15] S. Khuller, A. Malekian, and J. Mestre, "To fill or not to fill," *ACM Trans. Algorithms*, vol. 7, no. 3, pp. 1–16, 2011.

[16] A. D. Rodrigues and M. M. D. C. Cruz, "A generic decision model of refueling policies: A case study of a Brazilian motor carrier," *J. Transp. Literature*, vol. 7, no. 4, pp. 8–22, 2013.

[17] Y. Kobayashi, N. Kiyama, H. Aoshima, and M. Kashiyama, "A route search method for electric vehicles in consideration of range and locations of charging stations," in *Proc. IEEE Intell. Vehicles Symp. (IV)*, Jun. 2011, pp. 920–925.

[18] S. Storandt and S. Funke, "Cruising with a battery-powered vehicle and not getting stranded," in *Proc. 26th Conf. Artif. Intell. (AAAI)*, 2012, pp. 1–7, Accessed: Jun. 20, 2016. [Online]. Available: http://www.aaai.org/ocs/index.php/AAAI/AAAI12/paper/view/4794

[19] S. Storandt, "Quick and energy-efficient routes: Computing constrained shortest paths for electric vehicles," in *Proc. 5th ACM SIGSPATIAL Int. Workshop Comput. Transp. Sci.*, pp. 20–25, 2012.

[20] O. J. Smith, N. Boland, and H. Waterer, "Solving shortest path problems with a weight constraint and replenishment arcs," *Comput. Oper. Res.*, vol. 39, no. 5, pp. 964–984, May 2012.

[21] G. Laporte and M. M. B. Pascoal, "Minimum cost path problems with relays," *Comput. Oper. Res.*, vol. 38, no. 1, pp. 165–173, Jan. 2011.

[22] T. M. Sweda and D. Klabjan, "Finding minimum-cost paths for electric vehicles," in *Proc. IEEE Int. Electr. Vehicle Conf.*, Mar. 2012, pp. 1–4.

[23] T. Wang, C. G. Cassandras, and S. Pourazarm. (2014). *Energy-aware Vehicle Routing in Networks with Charging Nodes*. Accessed: Nov. 9, 2014. [Online]. Available: http://www.nt.ntnu.no/users/skoge/prost/proceedings/ifac2014/media/files/0814.pdf

[24] T. Wang, C. G. Cassandras, and S. Pourazarm, "Energy-aware vehicle routing in networks with charging nodes," 2014, *arXiv:1401.6478*. [Online]. Available: http://arxiv.org/abs/1401.6478

[25] G. Huber and K. Bogenberger, "Optimal charging strategies for electric cars on long trips," in *Proc. Conf. Future Automot. Technol.*, 2014, pp. 1–10.

[26] G. Huber and K. Bogenberger, "Long-trip optimization of charging strategies for battery electric vehicles," *Transp. Res. Rec., J. Transp. Res. Board*, vol. 2497, no. 1, pp. 45–53, Jan. 2015.

[27] Y. Wang, J. Jiang, and T. Mu, "Context-aware and energy-driven route optimization for fully electric vehicles via crowdsourcing," *IEEE Trans. Intell. Transp. Syst.*, vol. 14, no. 3, pp. 1331–1345, Sep. 2013.

[28] P. Chen and Y. Nie, "Stochastic optimal path problem with relays," *Transp. Res. Procedia*, vol. 7, pp. 129–148, Aug. 2015.

[29] M. W. Fontana, "Optimal routes for electric vehicles facing uncertainty, congestion, and energy constraints," Ph.D. dissertation, Sloan School Manage., Massachusetts Inst. Technol., Cambridge, MA, USA, 2013.

[30] J. A. Oliva, C. Weihrauch, and T. Bertram, "Model-based remaining driving range prediction in electric vehicles by using particle filtering and Markov chains," in *Proc. World Electr. Vehicle Symp. Exhib. (EVS27)*, Nov. 2013, pp. 1–10.

[31] S. Mehar, S. M. Senouci, and G. Remy, "EV-planning: Electric vehicle itinerary planning," in *Proc. Int. Conf. Smart Commun. Netw. Technol. (SaCoNeT)*, Jun. 2013, pp. 1–5.

[32] E. S. Rigas, S. D. Ramchurn, N. Bassiliades, and G. Koutitas, "Congestion management for urban EV charging systems," in *Proc. IEEE Int. Conf. Smart Grid Commun. (SmartGridComm)*, Oct. 2013, pp. 121–126.

[33] C. Xie and N. Jiang, "Relay requirement and traffic assignment of electric vehicles," *Comput.-Aided Civil Infrastruct. Eng.*, vol. 31, no. 8, pp. 580–598, Aug. 2016.

[34] S. A. Birrell, A. McGordon, and P. A. Jennings, "Defining the accuracy of real-world range estimations of an electric vehicle," in *Proc. 17th Int. IEEE Conf. Intell. Transp. Syst. (ITSC)*, Oct. 2014, pp. 2590–2595.

[35] M. R. Garey and D. S. Johnson, *Computers and Intractability: A Guide to the Theory of NP-Completeness* (A Series of Books in the Mathematical Sciences). 27th ed. New York, NY, USA: Freeman, 2009.

[36] R. Bellman, "The theory of dynamic programming," *Bull. Amer. Math. Soc.*, vol. 60, pp. 503–515, 1954, Accessed: Jun. 27, 2016. [Online]. Available: http://www.ams.org/journals/bull/1954-60-06/S0002-9904-1954-09848-8/

[37] E. Q. V. Martins, "On a multicriteria shortest path problem," *Eur. J. Oper. Res.*, vol. 16, no. 2, pp. 236–245, 1984.

[38] M. Ehrgott, *Multicriteria optimization*, 2nd ed. Berlin, Germany: Springer, 2005.

[39] P. Hansen, "Bicriterion path problems," in *Multiple Criteria Decision Making Theory and Application* (Lecture Notes in Economics and Mathematical Systems), vol. 177, M. Beckmann, H. P. Künzi, G. Fandel, and T. Gal, Eds. Berlin, Germany: Springer, 1980, pp. 109–127.

[40] T. Schreiter, H. van Lint, M. Treiber, and S. Hoogendoorn, "Two fast implementations of the adaptive smoothing method used in highway traffic state estimation," in *Proc. 13th Int. IEEE Conf. Intell. Transp. Syst.*, vol. 57, Sep. 2010, pp. 1202–1208.

[41] M. Treiber and D. Helbing, "Reconstructing the spatio-temporal traffic dynamics from stationary detector data," in *Cooperative Transport Dynamics*. Zürich, Switzerland: ETH Zurich, 2002, p. 3. [Online]. Available: https://tu-dresden.de/bu/verkehr/ivw/forschung/publikationen-fis/document_view?fis_type=publikation&fis_id=h299&set_language=en

[42] J. van Lint, "Empirical evaluation of new robust travel time estimation algorithms," *Transp. Res. Rec., J. Transp. Res. Board*, vol. 2160, no. 1, pp. 55–59, 2010.

[43] BMW. *BMW i3: Technische Daten*. BMW AG. Accessed: Jun. 27, 2016. [Online]. Available: http://www.bmw.com/com/de/newvehicles/i/i3/2015/showroom/technical_data.html

Gerhard Huber received the B.S. and M.S. degrees in mathematics from the Technical University of Munich, Germany, in 2010 and 2012, respectively, and the Ph.D. degree in traffic engineering in 2017, his work focuses on routing algorithms for battery electric vehicles.

From 2012 to 2016, he was working as a Research Associate with the Chair of Traffic Engineering with the University of the Federal Armed Forces Munich. From 2016 to 2019, he worked with DriveNow GmbH & Company KG as a Data Analyst in the area of carsharing. In summer 2019, he joined Sixt SE as a Data Scientist, again working on carsharing topics.

Klaus Bogenberger received the Diploma degree in civil engineering and the Ph.D. degree in traffic engineering from Technical University Munich, Germany, in 1996 and 2001, respectively. He was a Research Engineer with the BMW Group from 2001 to 2008. At first, he was responsible for the topics Traffic Flow Theory and Models, Department of Science and Transportation, and later on, he worked with the Department of Corporate Quality. From 2008 to 2011, he was the Managing Director and a Partner of the TRANSVER GmbH (Consultant Office for Transport Planning and Traffic Engineering) in Munich and Hannover. In 2012, he has been appointed by the University of the Federal Armed Forces Munich as a Professor for Traffic Engineering. Since 2020, he has been leading the Chair of Traffic Engineering and Control with the Technical University of Munich. His main research interests include among others car sharing systems, quality of traffic information, and autonomous vehicles.

Hans van Lint was born in Delft, The Netherlands, in 1971. He received the B.S. and M.S. degrees in civil engineering from the Delft University of Technology (DUT) in 1997, and the Ph.D. degree in freeway travel time prediction from the Transport and Planning Department, Civil Engineering and Geosciences Faculty, DUT, in 2004. Before his Ph.D. degree, he worked as Software Developer and a Project Engineer. Nine years after graduating, he was awarded an Antonie van Leeuwenhoek full professorship by the DUT Board of directors. His research interests include the interface of traffic flow theory, data assimilation, and analytics. He is/was supervisor of 21 Ph.D. students of which nine meanwhile (successfully) finished. As director of the Data Analytics and Simulation Lab he works, with his students and colleagues, on complex problems that involve multimodal traffic demand and supply estimation, prediction, and simulation. He wrote 67 journal articles and more than 100 peer-reviewed conference papers, and is active in many international projects. He served as Associate Editor of the IEEE TRANSACTIONS ON INTELLIGENT TRANSPORTATION SYSTEMS (T-ITS) and on the Editorial Board of Tr-Res Pt C and on various TRB committees.